Federal State Unitary Enterprise
State Scientific Centre
Research Institute of Atomic Reactors

Results of VVER-1000 Fuel Rod Simulator Tests under Core Reflood Conditions

A. V. Goryachev, I. V. Kuzmin, A. Yu. Leshchenko,
V. V. Serebryakov, V. P. Smirnov, A. S. Khrenov

2007

Introduction

Core reflooding under beyond the design-basis LOCA is considered as one of the ways to keep fuel within the VVER vessel and to prevent radiation impact on the environment. However, thermo-mechanical stresses appearing in the cladding and fuel rod columns as a result of fast cooling can cause cracking of the cladding and even its fracturing. It leads to fission product (FP) release from fuel, additional oxidation of claddings and fuel, generation of large amount of hydrogen and possible formation of explosive hydrogen-air mixture in the containment. This phenomenon was revealed in the test of single fuel rod simulators with cladding from Zircaloy and E110 [1, 2] as well as for model bundle tests performed at the QUENCH facility (FZK) under severe LOCA conditions [3]. The numerical modeling of the fuel rod behavior at the reflood stage is complicated due to the lack of experimental data on the character of mechanical damages of the oxidized claddings and FP release.

The experiments are aimed at obtaining data on the character of fuel rod cladding damage, hydrogen generation and FP release to develop a mechanistic model describing the behavior of the VVER-1000 fuel rods with a burnup of 50-60 MW·d/kg U under severe LOCA conditions. It will allow upgrading and improvement of computer codes and physical models developed for PWR as applied for VVER.

This paper describes the experiments with irradiated and unirradiated VVER fuel rod simulators to determine the hydrogen production and FP release in the core under reflooding as well as to reveal main factors causing additional cladding oxidation (oxidation of recovered ZrO_2 layer and oxidation of brittle crack surfaces). Obtained results are in good coincidence with FZK data for unirradiated simulators with Zircaloy and E110 claddings under the same conditions.

Results of the tests with irradiated simulators showed high hydrogen production as compared with unirradiated simulators under the same conditions. At high oxidation degree longitudinal cracks were revealed in the claddings of irradiated simulators even prior to quenching that caused an increased amount of hydrogen both at the preliminary oxidation and at the quench stage.

1. Samples and test rig

Fuel rod simulators shown in Fig.1 were used as samples. To make irradiated simulators, segments of spent VVER-1000 fuel rods 150 mm long were used. Fuel was removed from the segments edges and end components (top plug and fuel column stopper made from E110 alloy) were welded by argon-arc welding. The stopper is made in the form of a plug with a hole to simulator purging. The top plug is intended to fix the simulator on the hanger by means of a threaded joint. It has an axial channel for a tungsten-rhenium

thermocouple installation into the central channel of the fuel column at a distance of 77 mm from the sample lower end.

The unirradiated simulator of the same design has the cladding made from the E110 alloy and filled with unirradiated uranium dioxide pellets. The cladding length is 150 mm, outer diameter – 9.15 mm and wall thickness – 0.69 mm. The pellet outer diameter is 7.56 mm; the central hole diameter is 2.4 mm. In some cases the unirradiated simulators were equipped with three platinum-rhodium thermocouples fixed on the cladding at distances 27 mm, 77 mm and 127 mm from the sample lower end.

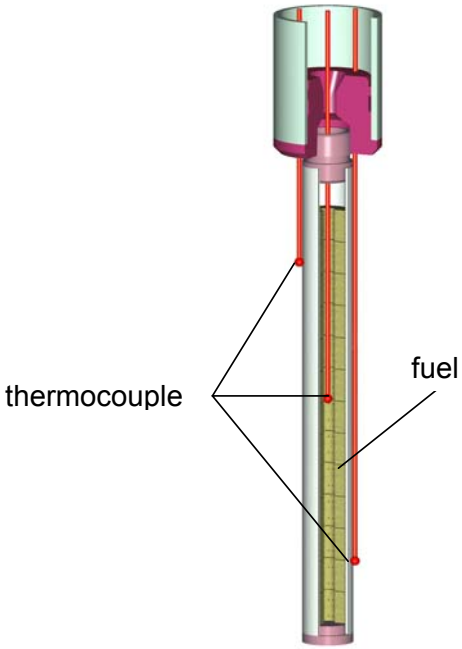

Fig. 1. Simulator layout.

Simulator test includes the following phases:

- Preliminary oxidation of the cladding in the steam flow to simulate fuel rod oxidation at the core drying stage under LOCA.
- Heating of the simulator up to the desired test temperature (1400 – 1700 °C).
- Simulation of core re-flooding by immersing the simulator into water with the given speed.

Figure 2 presents the furnace layout. The simulator is placed vertically in the centre of the working channel made from an alumina tube. The channel is placed in a split tubular molybdenum heater surrounded with screens and thermal insulation. The sample is fixed on the hanger, of which lower part is made from a zirconium tube covered with heat-resistant glass-like material to prevent its oxidation. The hanger was located in a drive controlled by a stepping motor and was moved through a sealing. The re-flooding conditions were simulated by a quick (within 1 s) movement of the simulator into a quenching tank down to the water surface and its further immersion into water at a speed of 15 mm/s. The water temperature in the quenching tank is held at 90 °C.

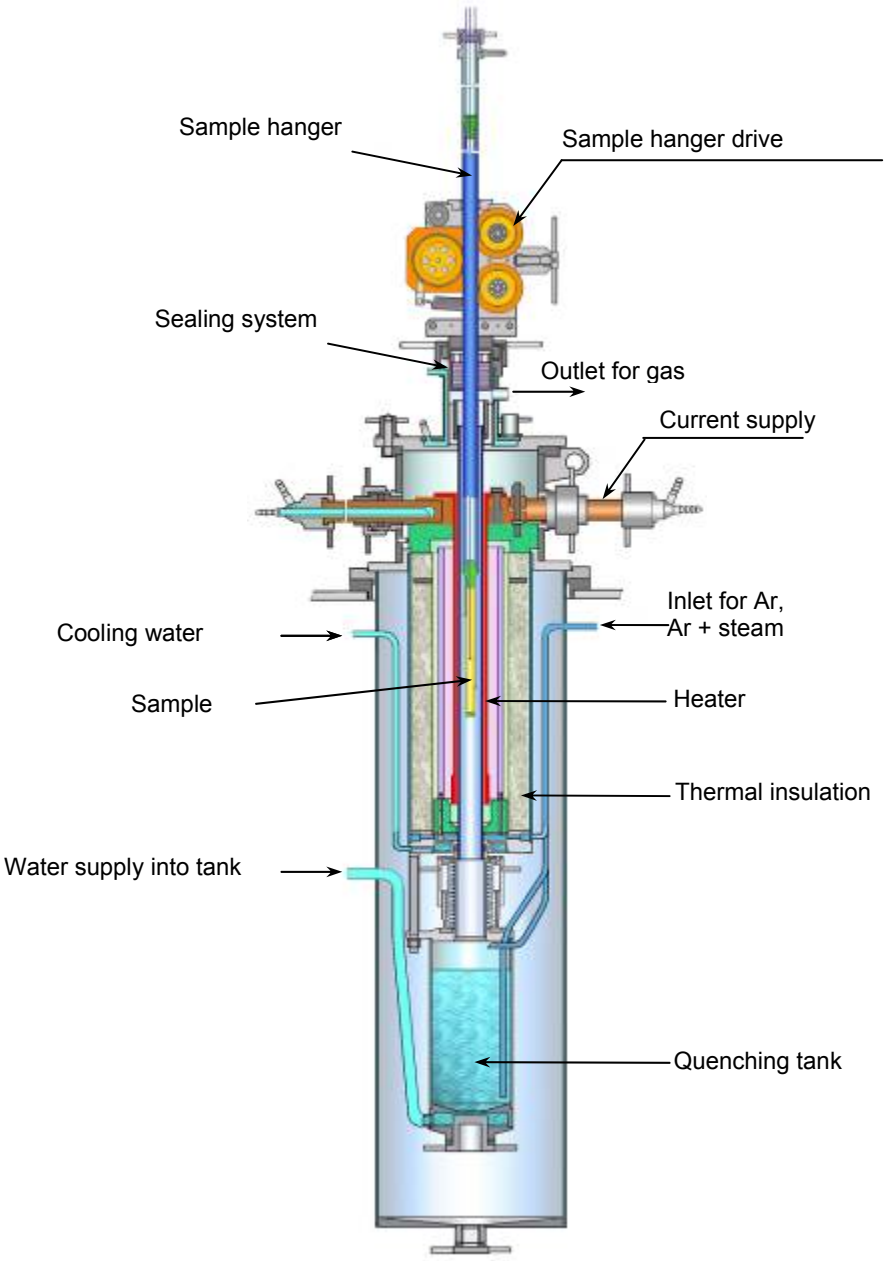

Fig.2. Test rig.

The gas pipeline system of the test rig performs the following functions [4, 5]:

- purges either inert carrier gas (argon) or argon-steam mixture through the working channel at the preliminary oxidation stage;
- purges inert gas through the simulator cavity to register the GFP release;
- transports generated hydrogen and released GFP to the measurement devices by means of inert carrier gas;
- maintains positive gas pressure drop between the heater cavity and working channel space to prevent the hydrogen and GFP leak and to protect the heater from steam;
- changes the direction of the gas flow to separate the hydrogen and GFP release at different experimental stages.

The main parameters measured during the tests with unirradiated simulators were: simulator temperature, gas flow rate and hydrogen concentration at the preliminary oxidation and the quench stage. Gamma-spectrometry and mass-spectrometry are additionally used in the tests with irradiated simulators to measure on-line GFP release from fuel. Also gamma-spectrometry is used to determine cesium concentration in the quenching tank water after the test.

2. Results of hydrogen production measurement during unirradiated simulator tests.

To evaluate relation of the amount of hydrogen generated during the simulator quench depending on the oxide film thickness on the cladding outer surface two series of the unirradiated VVER-1000 fuel rod simulators tests were performed at the quench temperatures of 1400 °C and 1700 °C. The experimental parameters and test results are presented in Table 1. A part of simulators was preliminary oxidized in the argon-oxygen medium at 1400 °C and the other part was preliminary oxidized in the argon-steam mixture at the same temperature. In the majority of experiments with preliminary oxidation in the argon-steam mixture, steam in the working channel was changed into argon before the desired heating temperature being achieved. The change of medium stopped the hydrogen generation. The simulator was quenched when the hydrogen concentration at the heating module outlet decreased up to the background value (Fig. 3).

At temperature of 1400 °C the hydrogen generation decreased during quenching with increasing of oxide film thickness (Fig. 4). The hydrogen production values for the simulators with the same oxide film thickness (~100 μm) coincide within the measurement error. All the simulators were intact and did not have any visible cracks on the cladding surfaces. The comparison of the obtained data with the results of the similar tests performed at FZK (Fig. 4)

proves a good coincidence of the results. Results of metallographic examination showed no oxidation of the cladding inner surface.

At temperature of 1700 °C a part of simulators quenched in water fractured. When quench began, a sharp fuel centerline temperature escalation up to 70 °C was observed during the first several seconds. It was related to a sharp intensification of the steam-zirconium reaction during quenching. A net of fine cracks was observed on the simulators claddings after quenching (Fig.5). A typical oxide structure observed on the cladding surface is shown in Figure 5. The metallographical results revealed a dense oxide film formed on the cladding outer surface and a lot of thin cracks in the metal layer. No oxidation was observed on the cladding inner surface. Hydrogen production for samples quenched from 1700 °C depends greatly on the maximum temperature and sample state after the experiment. Probably, it is conditioned by the character of damages of the sample at the quench phase.

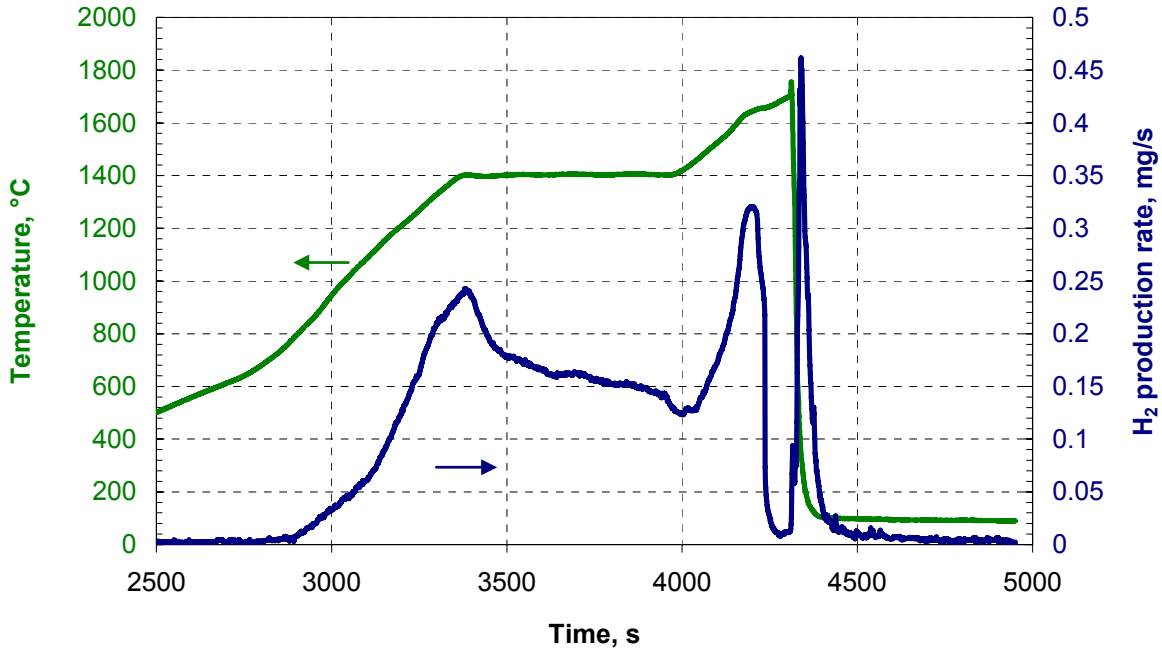

Fig. 3. Typical temperature history and hydrogen production rate for sample quenched at temperature of 1700 °C (simulator 32).

Table 1

Results of unirradiated simulator tests

Quench temperature, °C	1400												1700									
Simulator No.	21			22	23		24			35			25	26			27		28	31		32	
Oxidation time at 1400 °C, s	200			360	360		360			240			240	240			240		240	0		600	
Temperature during gas flow change before quench, °C	-			-	-		-			1400			-	1600			1600		1600	1650		1650	
Preliminary oxidation medium	O_2 - Ar			O_2 - Ar	O_2 - Ar		O_2 - Ar			Ar- steam			Ar-steam	Ar- steam			Ar- steam		Ar-steam	Ar- steam		Ar- steam	
Quenching medium	water			water	water		water			water			water	water			steam		steam	water		water	
Pellets	UO2			UO2	UO2		UO2			UO2			UO2	UO2			no		no	UO2		UO2	
Max temperature during quench, °C													1717	1722			1704		1703	1770		1755	
Simulator state after test	Non-fractured			Non-fractured	Non-fractured		Non-fractured			Non-fractured			fractured	Non-fractured			Non-fractured		Non-fractured	fractured		fractured	
Total hydrogen production, mg	-			-	-		-			103 ± 8			238 ± 19	187 ± 15			140 ± 11		166 ± 14	153 ± 12		226 ± 18	
Hydrogen production during quench, mg	7.2 ± 0.6			3.5 ± 0.3	3.4 ± 0.3		2.7 ± 0.2			3.2 ± 0.3			14.1± 1.1	8.6± 0.7			11.6 ± 0.9		6.6 ± 0.5	27.4 ± 2.2		17.5 ± 1.4	
Weight gain, g	0.353			0.596	0.912		0.973						-	1.5239			1.11675		1.2585	-			
Average oxide film thickness (by weight gain), μm	38			64	98		105							165			120		135				
Section coordinate	27	77	127		27	127	27	77	127	27	77	127	80	27	77	127	77	141	77	27	75	27	77
ZrO_2 average thickness, μm	18	-	13		155	105	66	97	127	31	99	99	251	67	144	98	52	83	124	100	140	214	288
α-Zr(O) average thickness, μm	69	103	103		180	116	143	163	137	35	146	146		243	347	111	370	160		247			
Metal layer thickness, μm	685	692	703		605	629	656	625	618	686	636	647	530	676	614	634	668	656	619	650	636	556	508

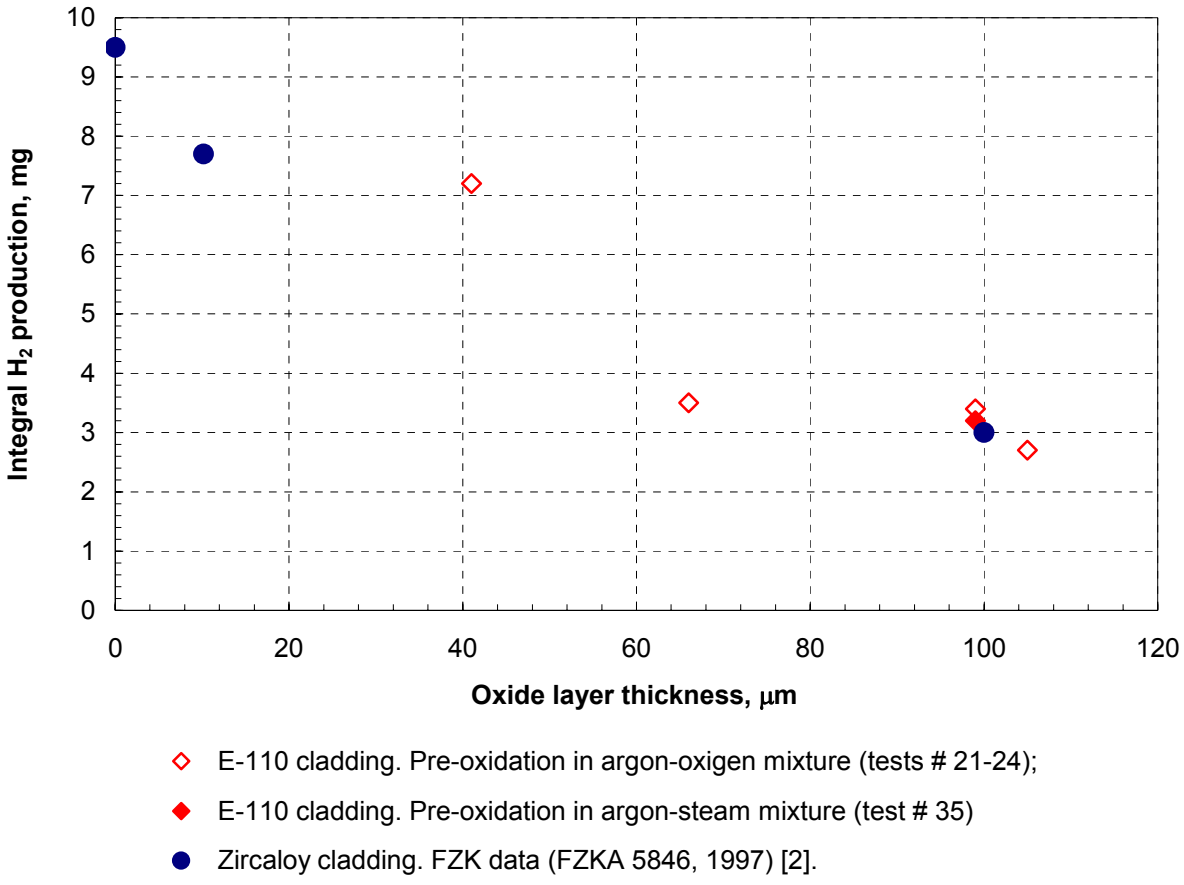

Fig. 4. Hydrogen production vs. oxide film thickness at 1400 °C. Comparison with FZK results.

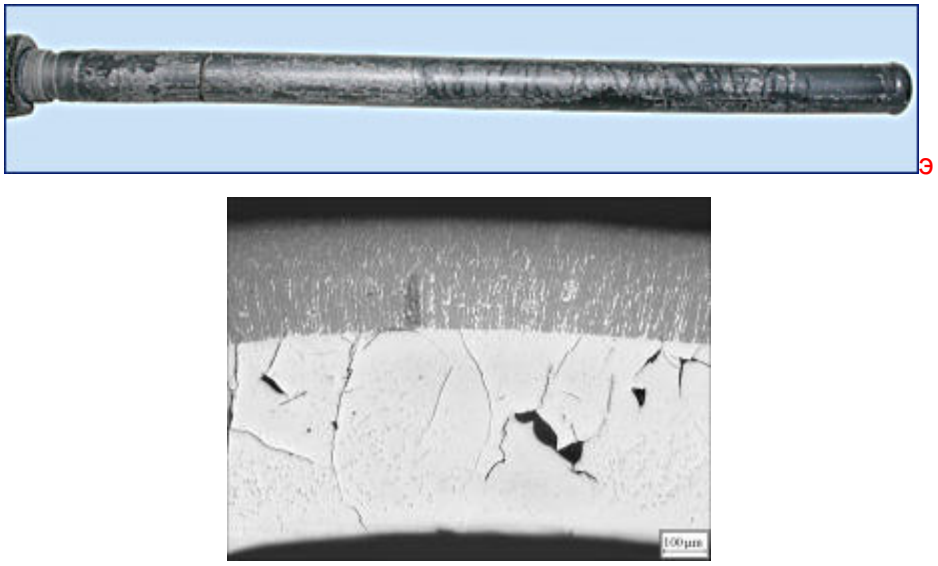

Fig. 5. Appearance and structure of the simulator cladding after quench at temperature of 1700 °C (simulator 32).

3. Results of hydrogen production measurement during irradiated simulator tests.

The matrix of experiments performed with irradiated VVER-1000 fuel rod simulators is presented in Table 2.

Table 2

Parameters of irradiated simulators tests

Oxide film thickness, μm \ Quench temperature, °C	**1400**	**1600**	**1700**
0	2 tests	2 tests	2 tests
100	2 tests	1 test	1 test
300	2 tests	1 test	

Experiments with zero oxide film thickness were performed in the inert medium, the carrier gas flow being directed top-bottom though the working channel. Before quenching the samples subjected to preliminary annealing within 240 s at 1400 °C in the inert medium. This procedure ensured the same temperature regime of the test as for the pre-oxidized samples with an oxide film thickness of 100 μm to so as to compare the GFP release kinetics.

In the quench tests with simulators with oxide films about 100 μm and 300 μm thick, the samples were pre-oxidized in the argon-steam medium at 1400 °C within 240 s and 1100 s, respectively. Carrier gas flow was directed bottom-top through the working channel at preliminary oxidation phase. Then steam supply was stopped and the simulator was heated up to the required temperature. Just before quench, the carrier gas flow was directed vice versa. It allowed the separation of hydrogen generated at the preliminary oxidation stage from that one generated during the quench phase. Figures 6 and 7 present the typical temperature history, hydrogen production rate and post-test appearances of simulators (Fig. 8 as well). The test parameters and results are given in Table 3. Figure 9 presents the typical structure of simulators claddings after the test. The main difference in the structure of irradiated claddings from unirradiated ones with low oxidation degree is the presence of an inner α-zirconium layer stabilized with oxygen formed as a result of cladding-fuel pellet interaction (Fig. 4).

Only samples with zero oxide film and simulators with the oxide film thickness of 100 μm and quenching temperature of 1400 °C was intact when removed from the test rig (Fig. 6). Other simulators fractured into several fragments at pellet-to-pellet interfaces apparently at the quench stage. Longitudinal cracks with highly oxidized surfaces were revealed on the cladding of these fragments (Fig. 7-8). High oxidation of the longitudinal crack surfaces and absence of oxidation of the transversal fracture surfaces proves

longitudinal cracks formation before the change of the working channel medium into inert gas.

The fuel pellets, spilled from the fractured claddings, disintegrated into several fragments up to 10 mm in size (Fig. 7).

The increasing hydrogen production rate after ~500 s of pre-oxidation at 1400 °C proves the intensification of oxidation (Fig. 7 as compared to Fig. 6). This phenomenon can be explained by cracking of the simulator and generation of new cladding surfaces (longitudinal crack edges, clad inner surface) that can be oxidized in steam. Intensive oxidation of the cladding inner surface adjacent to longitudinal cracks caused their additional deformation and, probably, became the cause of the cladding fragmentation observed on the quenched simulators.

.

Fig. 6. Temperature history and hydrogen production rate for the test 39. Appearance of the simulator 39 after the test. (100 μm and quench at 1400 °C).

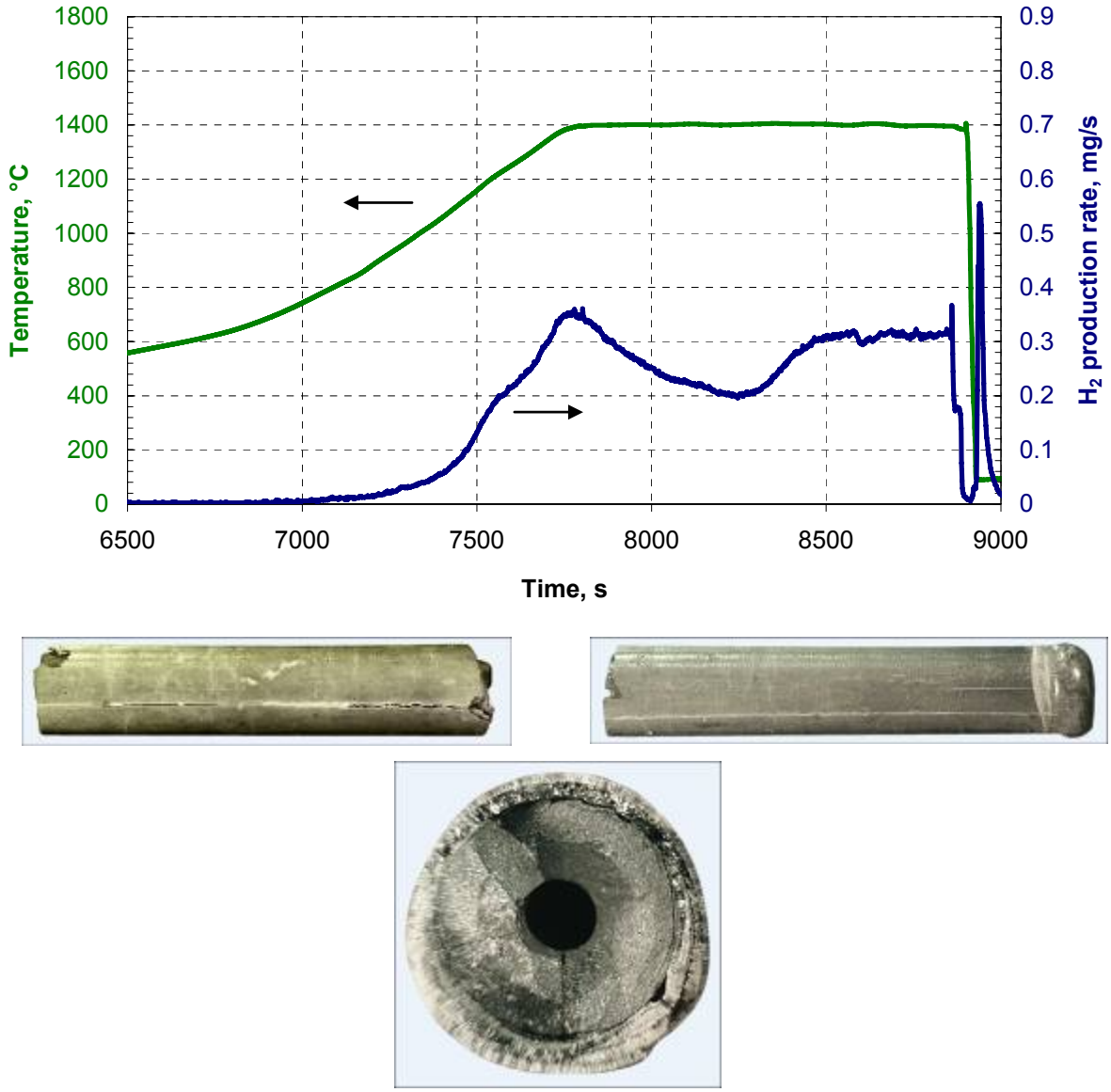

Fig. 7. Temperature history and hydrogen production rate for the test 55. Appearance and fuel fragments of the simulator 55 after the test. (300 μm and quench at 1400 °C).

Fig. 8. Fragments of simulator 53
(100 μm and quench at 1700 °C).

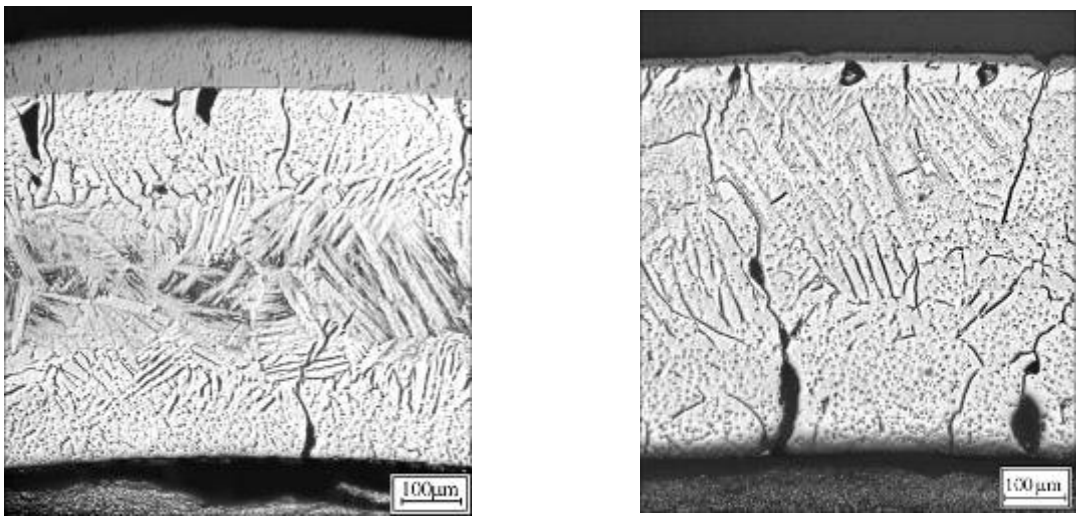

a b

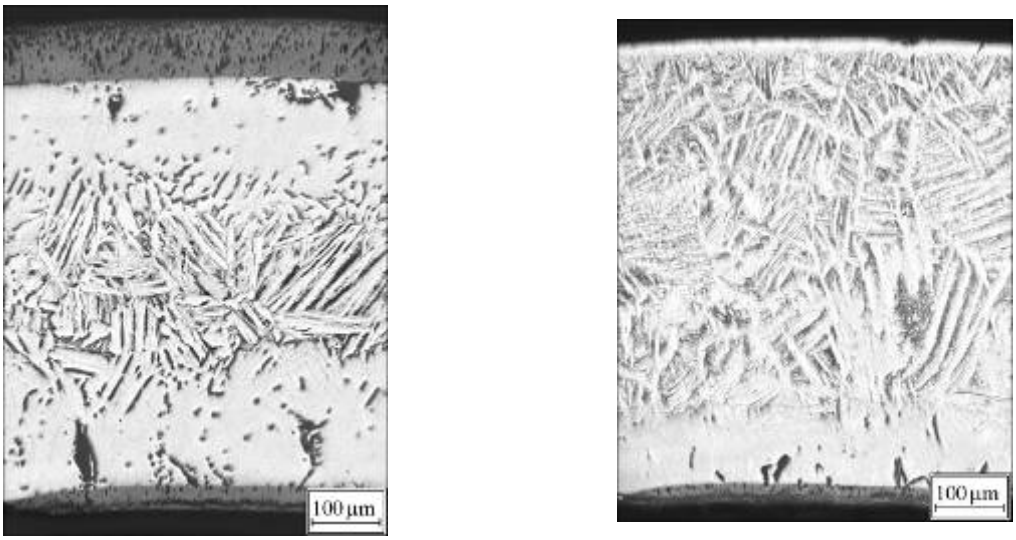

c d

Fig. 9. Structure of irradiated simulator cladding after the test:
a - simulator 36; b – simulator 37; c – simulator 39; d – simulator 40.

Table 3

Hydrogen production during experiments with irradiated fuel.

Experiment No.	**36**	**37**	**39**	**40**	**45**	**46**	**47**	**49**	**51**	**53**	**54**	**55**	**56**
Burnup, MW·d/kg U	54	54	65	65	65	65	65	65	65	65	65	65	65
Oxidation time at 1400°C, s	240		240						240	240	1050	1100	1100
Gas medium	Ar-steam	Ar	Ar-steam	Ar	Ar	Ar	Ar	Ar	Ar-steam	Ar-steam	Ar-steam	Ar-steam	Ar-steam
Temperature at the onset of quench, °C	1400	1700	1400	1400	1600	1400	1600	1700	1600	1700	1400	1400	1600
Max temperature at the quench stage, °C	1407	1703	1428	1411	1604	1422	1604	1706	1658	1846	1419	1406	1601
Final sample state	3	2	2	3	2	3	3	2	1	1	1	1	1
Oxide film thickness, μm	111	19	92	9	14	8	17						
Thickness of outer α - Zr(O) layer, μm	186	31	126	23	41	26	43						
Thickness of inner α - Zr(O) layer, μm	170	337	122	90	75	113	191						
Metal layer thickness, μg	607	648	614	674	696	696	676						
Total hydrogen production, mg	164 ± 13	16.3 ± 1.3	173 ± 14	13.6 ± 1.1	20.6 ± 1.6	9.4 ± 0.6	20.5 ± 1.6	26 ± 2	210 ± 17	252± 20	386± 31	497± 40	686± 55
Hydrogen production during quench, mg	6.7 ± 0.5	14.7 ± 1.2	7.0 ± 0.6	13.6 ± 1.1	20.6 ± 1.6	9.4 ± 0.6	20.5 ± 1.6	26 ± 2	22.46 ± 1.8	39.16 ± 3.1	13.96 ± 1.1	17.16 ± 1.4	43.2 ± 3.5

Sample state after experiment:
1 – sample cracked after the test
2 – sample cracked during post-test operations
3 – sample did not crack

Thus, the longitudinal crack formation could occur at the isothermal pre-oxidation stage of the test and be the result of stresses appearing in the cladding due to increasing oxide film thickness. The intensification of cladding cracking can be also caused by stresses resulted from the difference in the thermal expansion coefficients of fuel and cladding during the pre-oxidized simulator heating.

Figure 10 shows the hydrogen production versus oxide film thickness and quench temperature. The hydrogen production increases with the rise of the quench temperature. Such increase is related to a larger amount of longitudinal cracks that enlarge the cladding surface under oxidation. The low hydrogen productions observed for the simulators with the oxide film 100 μm thick and quench temperature of 1400 °C is attributed by the absence of longitudinal cracks and protective effect of the dense film on the cladding surface. It should be mentioned that fuel oxidation of simulators with fractured cladding can also contribute to the increased hydrogen production. Unlike to non-fractured simulators, the inert gas protecting fuel from oxidation could flow out through the cladding cracks, thus allowing steam to contact with fuel.

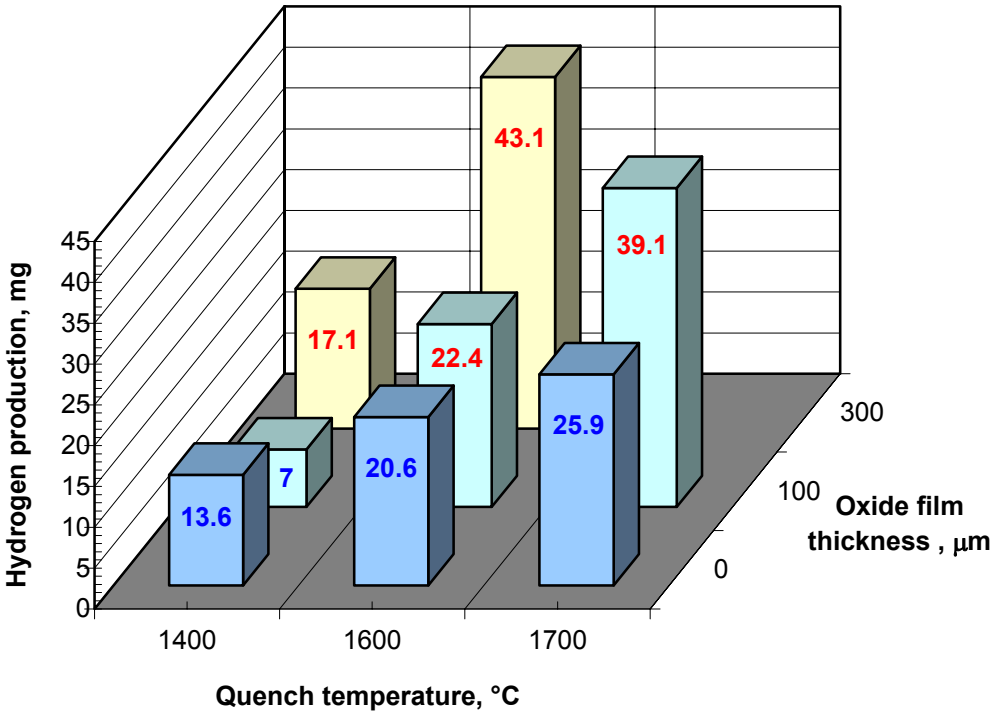

Fig. 10. Maximum hydrogen production during quench.

4. Results of FP release measurement in experiments with irradiated VVER-1000 fuel rod simulators

To evaluate the GFP release rate, the gas pipeline comprises a gas flow meter, ^{85}Kr gamma-activity detection unit and mass-spectrometer. The ^{85}Kr gamma-activity detection unit is a section of the carrier gas line wired spirally on the gamma-detector. Based on the registered intensity of the ^{85}Kr gamma-line with energy 514 keV, the rate and amount of ^{85}Kr released during the experiment is calculated. The mass-spectrometer is used to measure the non-radioactive xenon concentration in the carrier gas. The technique for determination of the GFP release is described in refs. [4, 5]. The ^{85}Kr and Xe release measured during the experiment is shown in table 4. The typical kinetics of the GFP release during the experiment is shown in Fig. 11, 12. As for experiments 54, 55 and 56 with long-term isothermal annealing, the ^{85}Kr release rate decreased monotonously, that evidenced about absence of fuel oxidation in spite of the formation of longitudinal cracks causing the increased hydrogen production.

Figure 13 shows the relative ^{85}Kr release during the whole experiment versus isothermal annealing time and quench temperature. The presented values are averaged by the results of samples test under the same conditions. The Kr release increases with the increasing time of the isothermal annealing and quench temperature. The Kr release during quench phase also increases as the quench temperature rises.

To evaluate the relative FP release, the initial FP content in fuel was determined by dissolving the reference fuel samples. Several fuel samples selected from the tested simulators were also dissolved to evaluate the relative FP release. Table 4 presents the relative ^{85}Kr release from the fuel samples taken from the central part of simulator, where the temperature and, consequently, GFP release are maximal. Actually, the relative ^{85}Kr release determined during the experiments is averaged by the simulator length and is less than that one given in the dissolution data.

Table 4

Test parameters of irradiated fuel rod simulator and FP release.

Experiment No.		**36**	**37**	**39**	**40**	**45**	**46**	**47**	**49**	**51**	**53**	**54**	**55**	**56**
Burnup, MW·d/kg U		54	54	65	65	65	65	65	65	65	65	65	65	65
Annealing time at 1400°C, s		240	240	240	0	240	240	240	240	240	240	1050	1110	1110
Quench temperature, °C		1400	1700	1400	1400	1600	1400	1600	1700	1600	1700	1400	1400	1600
Max temperature during quench, °C		1407	1703	1428	1411	1604	1422	1604	1706	1658	1846	1419	1406	1601
Total ^{85}Kr release, μl		37 ±4	65 ±8	33 ±4	16 ±2	18 ±2	11 ±1	16 ±2	28 ±3	19 ±2	58 ±7	40 ±5	34 ±4	40 ±5
Total Xe release, μl		12.9 ±1.3	34 ±3.4	9.9 ±1.0	4.9 ±0.5	5.0 ±0.5	3.1 ±0.3	4.9 ±0.5						
Relative ^{85}Kr release, %		16.5 ±4.0	29.4 ±3.2	8.0 ±4.5	4.0 ±4.5	4.9 ±4.5	3.0 ±4.6	4.2 ±4.5	7.6 ±4.5	5.2 ±4.5	15.8 ±4.2	10.8 ±4.4	9.1 ±4.4	10.9 ±4.3
Relative ^{85}Kr release during quench, %		1.0 ±0.2	3.5 ±0.8	0.9 ±0.2	0.9 ±0.2	1.4 ±0.3	0.4 ±0.1	1.1 ±0.1	2.5 ±0.5	1.8 ±0.4	2.0 ±0.4	1.0 ±0.2	0.9 ±0.2	1.1 ±0.2
Relative ^{85}Kr release from the sample centre (dissolution data), %		18.8 ±4.0	42.3 ±2.7	12.7 ±4.3	2.2 ±4.8									
Average relative cesium release, %	^{137}Cs	5		9	3	14		8						
	^{134}Cs	-		11	3	14		10						
Relative cesium release into quenching tank water, %	^{137}Cs	0.6 ±0.2	1.2 ±0.3	1.3 ±0.3	0.6 ±0.2	0.9 ±0.2	0.4 ±0.2	1.1 ±0.3		0.8 ±0.2	0.9 ±0.2	1.9 ±0.4	1.4 ±0.2	0.9 ±0.2
	^{134}Cs	0.5 ±0.2	1.0 ±0.2	1.2 ±0.3	0.6 ±0.2	0.9 ±0.2	0.4 ±0.2	1.1 ±0.3		0.8 ±0.2	1.0 ±0.2	2.2 ±0.4	1.7 ±0.3	1.1 ±0.3

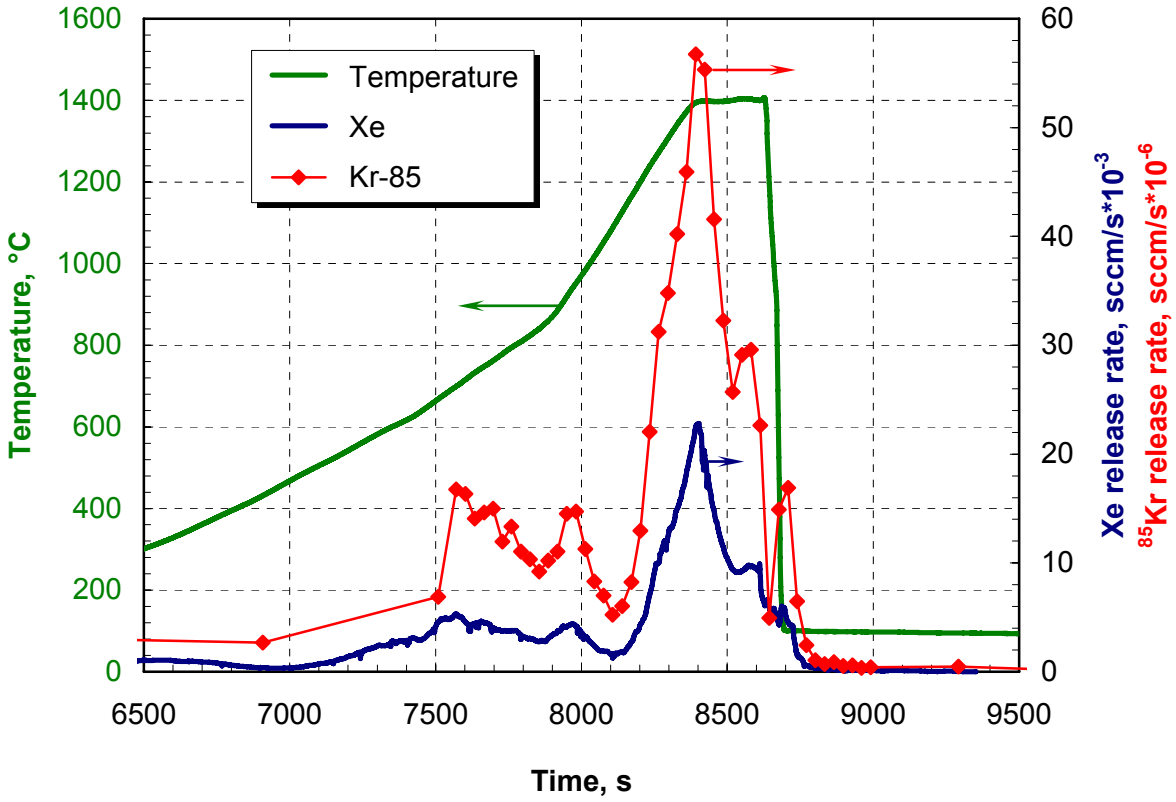

Fig. 11. ^{85}Kr and Xe release in experiment 36.

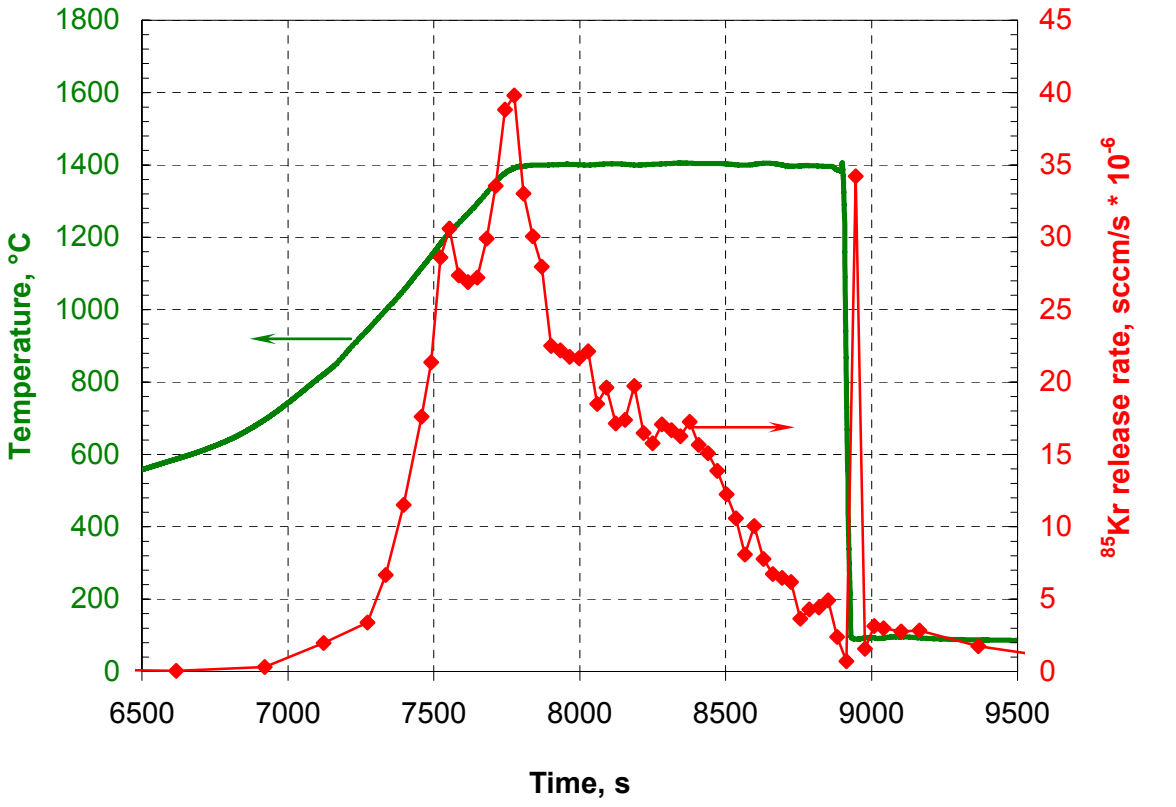

Fig. 12. ^{85}Kr release in experiment 55.

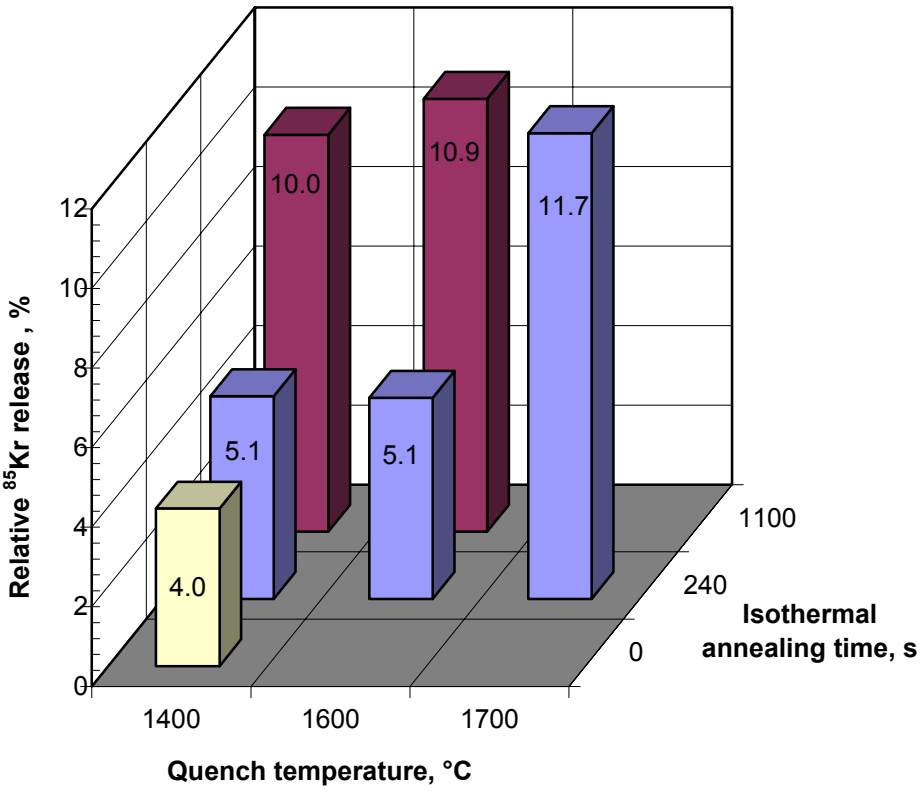

Fig. 13. Average values of relative ^{85}Kr release by several experiments

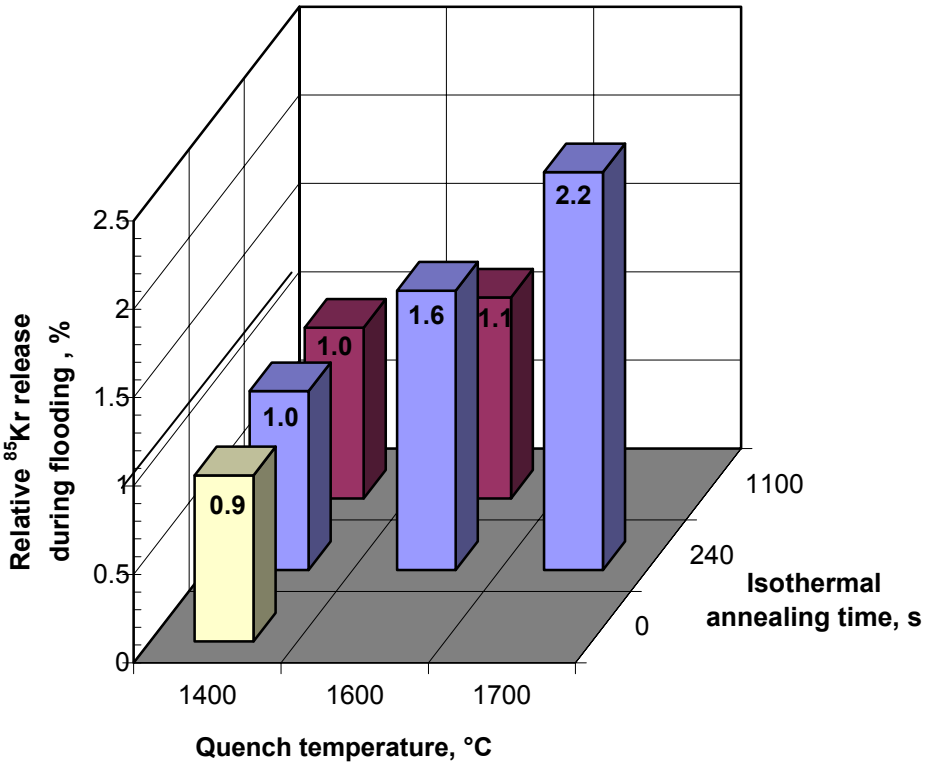

Fig. 14. Relative ^{85}Kr release during quench versus isothermal annealing time and quench temperature.

As for the non-fractures simulators (Table 4), the average relative cesium release was evaluated on the basis of pre- and post-test gamma-scanning (Fig. 15). Supposing that the cesium radial distribution before and after a test is equal, the average release can be evaluated by the relation of the registered cesium gamma-emission intensities integrated along the length. The scanning parameters – measurement geometry, detector efficiency, acquisition time of spectra– were not changed.

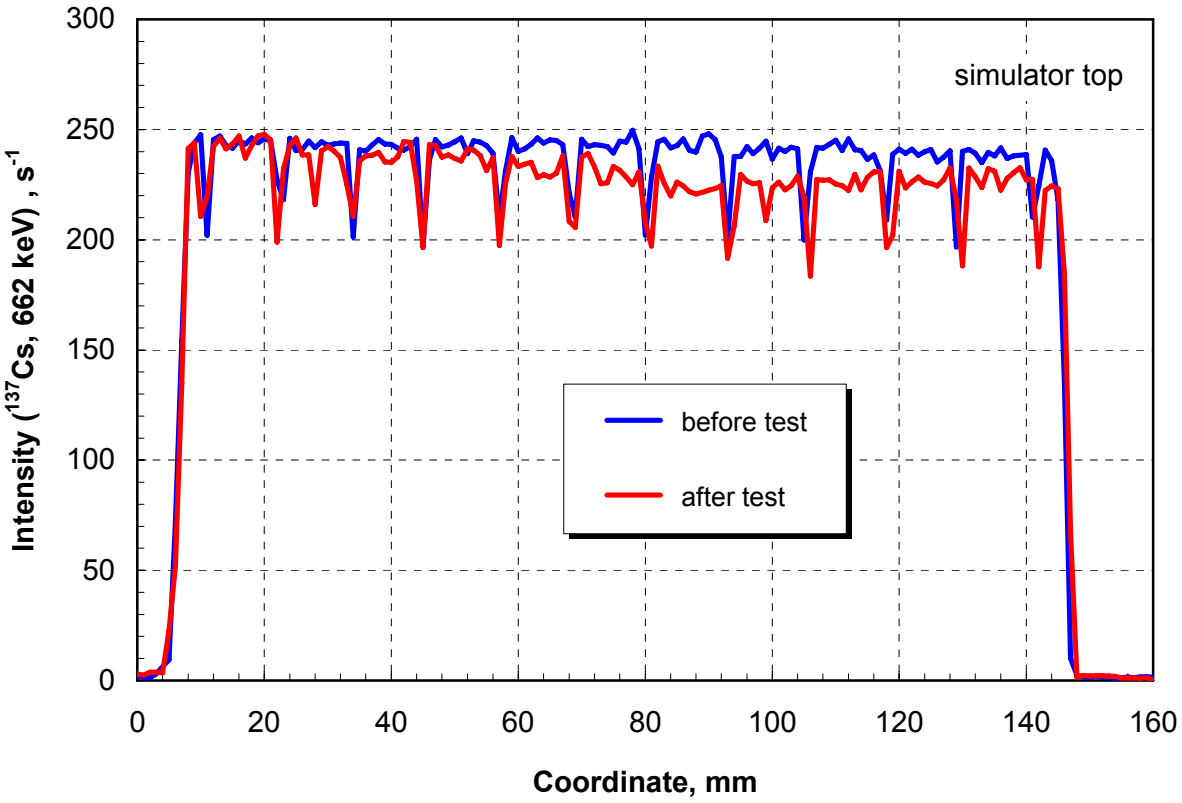

Fig. 15. Gamma-scanning results of simulator 36.

Water was sampled from the quenching tank before and after each experiment to determine the background and post-test FP content. Based on the gamma-spectrometry analysis of the quenching tank water samples the relative cesium release into water was calculated. The calculation was done on the basis of published data on the ^{137}Cs and ^{134}Cs accumulation in VVER-1000 fuel [6]. At a quench temperature of 1400 °C, the cesium release increases as the isothermal annealing time becomes longer and it decreases as the quench temperature rises.

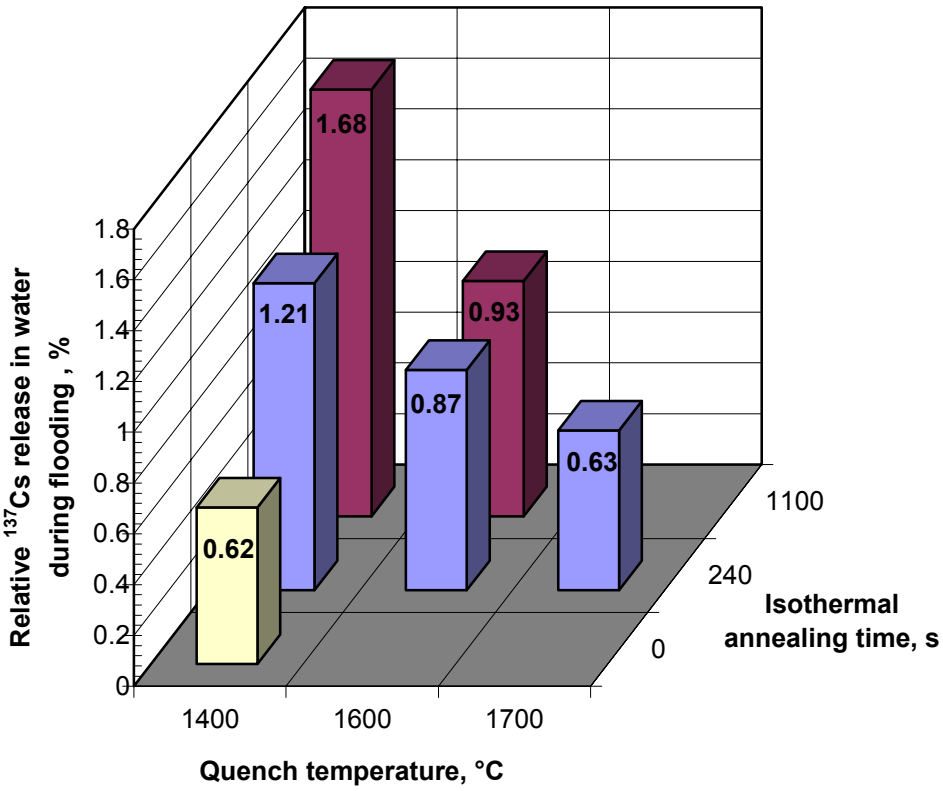

Fig. 16. Relative ^{137}Cs release during quenching versus isothermal annealing time and quench temperature

Conclusion

A series of experiments have been performed to study the behavior of irradiated and unirradiated VVER-1000 fuel rods under conditions simulating core reflooding under severe LOCA. The test included the following stages:

- Oxidation of the cladding in the steam flow to simulate the core drying stage under beyond the design-basis LOCA.
- Heating of the simulator up to the given test temperature.
- Simulation of core reflooding by immersing the hot sample into water at the given speed.

The experiments resulted in data on the state of fuel and simulator cladding with the oxide film 0-300 μm thick quenching with water from 1400 – 1700 °C. A data array was obtained on the hydrogen production, GFP and cesium release both at the preliminary oxidation of the simulator and during quench.

At a high oxidation level longitudinal cracks formation was revealed in the irradiated simulators claddings even prior to quenching that caused the increased hydrogen production both at the preliminary oxidation and quench stage. As for unirradiated simulators tests, no longitudinal cracks appeared.

The obtained data will be used for modeling VVER-1000 50-60 MW·d/kg U fuel rod behavior under severe LOCA.

References

1. J. Stuckert, M. Steinbrück, U. Stegmaier, “Single rod quench tests with Zr-1%Nb cladding. Comparison with Zircaloy-4 cladding tests and modeling”, FZKA 6604, 2001
2. P. Hofmann, V. Noack, M. S. Veshchunov et. al, "Physico-chemical behavior of Zircaloy fuel rod cladding tubes during LWR severe accident reflood", FZKA 5846, 1997
3. Status of the QUENCH Program at FZK \ M. Große, U. Stegmaier, L. Steinbock, M. Steinbrück \ Proceedings of the 11th International QUENCH Workshop, Forschungszentrum Karlsruhe, October 25-27, 2005
4. A. V. Goryachev, I. V. Kuzmin, A. Yu. Leshchenko , "Results of Unirradiated and Irradiated VVER Fuel Rod Simulator Tests under Reflood Conditions", Proceedings of the 12th International QUENCH Workshop, Forschungszentrum Karlsruhe, October 24-26, 2006
5. I. V. Kuzmin, A. Yu. Leshchenko, V. V. Serebryakov, A. V. Goryachev. Test rig and techniques for irradiated VVER fuel rod simulators tests under re-flood conditions // Proc. of FSUE SSC RIAR, 2007, P. 54–65
6. Radiation safety manual. V. F. Kozlov //, Energoatomizdat, 1999